Functional Drift of Sequence Attributes in the FK506-Binding Proteins (FKBPs)

Andrzej Galat*

Institute de Biologie et de Technologies de Saclay, DSV/CEA, CE-Saclay, F-91191 Gif-sur-Yvette Cedex, France

Received November 21, 2007

Diverse members of the FK506-binding proteins (FKBPs) group and their complexes with different macrocyclic ligands of fungal origins such as FK506, rapamycin, ascomycin, and their immunosuppressive and nonimmunosuppressive derivatives display a variety of cellular and biological activities. The functional relatedness of the FKBPs was estimated from the following attributes of their aligned sequences: 1° conservation of the consensus sequence; 2° sequence similarity; 3° pI; 4° hydrophobicity; 5° amino acid hydrophobicity and bulkiness profiles. Analyses of the multiple sequence alignments and intramolecular interaction networks calculated from a series of structures of the FKBPs revealed some variations in the interaction clusters formed by the AA residues that are crucial for sustaining peptidylprolyl cis/trans isomerases (PPIases) activity and binding capacity of the FKBPs. Fine diversification of the sequences of the multiple paralogues and orthologues of the FKBPs encoded in different genomes alter the intramolecular interaction patterns of their structures and allowed them to gain some selectivity in binding to diverse targets (functional drift).

INTRODUCTION

The FK506-binding proteins (FKBPs)[1] belong to a large superfamily of peptidylprolyl cis/trans isomerases (PPIases) which also contains[2,3] 1° the cyclophilins, 2° the Pin1/parvulin-like group of proteins, 3° trigger factors, and 4° the PP2A phosphatase activator.[4] The nominal mass of a small eukaryotic FKBP is around 12 kDa, whereas the largest FKBP (135 kDa) that modulates the growth cones of dorsal root ganglion neurons[5] consists one FK506-like binding domain (FKBD). Some large FKBPs may consist of up to four consecutive FKBDs and diverse sequence motifs such as the tetratricopeptide (TPR), calmodulin-binding domain (CBD), nuclear localization signal (NLS), leucine-zipper, EF-hand, transmembrane (TM) segment, and other motifs.[2] The FKBPs display a wide phylogenetic distribution, and variable numbers of their transcripts are expressed in the organisms at different levels of development.[2] Only several FKBPs have been isolated to homogeneity from natural sources,[6–8] whereas the majority of diverse sequences of the FKBPs discussed in this report were derived from cDNAs and diverse genome sequencing projects.[9–13] Diverse functional and biological features of the FKBPs and their cofactors have been described.[1–3,6–8,14–16,20–26]

Experimental data support the idea that a great majority of the FKBPs exhibit PPIase activity[1–3,16] whose in vivo significance remains obscure. Since the late 1980s, some members of the PPIase superfamily of proteins have been extensively studied because they bind to several immunosuppressive macrolides of fungal origin that can effectively suppress the immune system of patients with transplanted organs, namely cyclosporin A (CsA), FK506 (known also as tarcolimus), and rapamycin (known as sirolimus).[1,14–16] The potential of the FKBPs to bind different proteins creates a wide spectrum of cellular entities that may be targeted by the powerful and clinically useful immunosuppressants FK506, rapamycin, and their natural and synthetic derivatives.[14,17–19] The FKBPs localized to different cellular compartments could be under the control of these drugs which influence such processes as gain of tolerance toward transplanted organs,[1,2,16] inflammatory processes,[2,16] cell growth and proliferation processes,[2,16] neuron protection against ischemic shocks,[20–23] and many other cellular activities.

It could be tentatively suggested that the FKBPs encoded in different genomes have had to acquire some recognition selectivity that was imposed by a variety of intra- and extracellular ligands.[16,24–26] Target specificity and functions of the large FKBPs within diverse cellular entities should be also modulated by the other sequence motifs than the FKBDs themselves. In this communication, we have analyzed the 3D structures of the FKBDs and sequence repertoires of the FKBPs encoded in different genomes.[9–13,27,28] These analyses aimed at unraveling the sequence-structure diversity of the FKBDs derived from some subtle changes within the intramolecular interaction networks of the hydrophobic AA residues surrounding the PPIase cavity that has the capacity to bind diverse small molecules and proteins.[1–3,16]

METHODS

Databases and Sequence-Homology Searching Processes. Diverse genomic databases produced in the National Centre of Biotechnology Information, (NCBI http://ncbi.nlm.nih.gov) were used.[27] Also, the protein sequence databases assembled in the Protein Information Resources (PIR) databases (http://pir.georgetown.edu)[28] have been used in searches for diverse sequence motifs typical of the FKBPs.[29] Overall hydrophobicity (HI, expressed in percent) of proteins

* To whom correspondance should be addressed. Mailing address: Bat. 152, SIMOPRO/DSV/CEA, CE-Saclay, F-91191 Gif-sur-Yvette Cedex, France. Fax: 33-169089137. E-mail: galat@dsvidf.cea.fr.

10.1021/ci700429n CCC: $40.75
Published on Web 04/16/2008

was calculated as described[29,30] using a nine AA residues sliding frame and the Kyte−Doolittle hydrophobicity scale.[31,32]

Multiple Sequence Alignments and Their Analyses. The Data-SQ program[29] was used for selection of sequences of the FKBDs for multiple sequence alignments (MSA). MSAs were produced with the ClustalW60 program[33] using the Blosum30 AA exchange matrix[34] and a gap penalty of 10. The quality of the MSAs was assured using the following rules: For 1°, the MSAs were structured using the blocks of closely related sequences; for example, the orthologues and paralogues of the small FKBPs were used as the top block of sequences. For 2°, the MSAs were manually adjusted according to the interaction patterns obtained from the analyses of 3D structures, namely the canonical secondary structures, the AA residues that form the PPIase activity site, and the "aromatic/hydrophobic" networks were checked for proper alignments. The MSAs consisting N sequences were processed with a modified version of the Pola_SQ program[29] which produced N smaller-size MSAs that contained the sequences whose physicochemical attributes were similar, namely whose F_{ij} values[29] were not less than 0.75% of the highest F_{ij} value in given series of chosen FKBDs. The smaller-size MSAs (called here gradient maps of the AA substitutions) consist the sequences ordered according to the descending values of the IDs and F_{ij} values. The levels of residue (RC), sequence (SC), and motif (MC) conservation were estimated from the MSAs using the following three measures and the all-to-all pairwise comparison: 1° RCs, SCs, and MCs were calculated with the Valdar−Thornton formula;[35] 2° information entropy according to Shannon[36] at column j of a MSA for RC was calculated from the following equation (1),

$$\mathrm{Ie}_j = -\sum_{a=1}^{20} p_{ja} \log_2(p_{ja}) \tag{1}$$

where p_{ja} is the probability of the appearance of residue a at position j. 3° for chosen sequence fragments and sequence motifs of the aligned sequences, the SCs and MCs were calculated from the scoring function in Jensen−Shannon (JS) entropy[36] as formulated by Yoon and Levitt.[37] The levels of sequence conservation (RCs, SCs, and MCs) D and S are the averaged values derived from all the combinations of given sequence fragment or motif within the entire MSA. The following residues that have been proven to be crucial for the PPIase activity of the human archetypal FKBP12a and as those that form the typical sequence hallmark for the FKBP family of proteins[29] were used in calculation of the conservation levels within the PPIase cavity: Y26, F36, D37, F48, Q53, E54, V55, I56, W59, Y82, H87, I90, and F99. The AA residues shown in Table AT1 (Supporting Information Appendix 1.3) come from the sequence of hFKBP12a used as reference.

Analyses of 3D Structures. The coordinates of X-ray structures were selected from the Worldwide Protein Data Bank (wwPDB) (http://www.rcsb.org/pdb).[38] Diverse structures of the FKBPs at a resolution better than 3.3 Å were analyzed. A suite of programs (CORDAN_Prot) was derived from the CORDAN program[39] and was used for computing diverse geometry data from the PDB files.[38] The interatomic distance maps[40,41] were generated between all the atoms in the AA residues that are in $i \geq i + 2$ sequence positions. A 4.5 Å cutoff was used in distance computing. The distances (interactions) were sorted out into the following three types, namely 1° interactions between electron-donor and electron-acceptor atoms (diverse types of N and O atoms); 2° interactions between hydrophobic atoms (different types of C and S atoms); 3° interactions between the atoms in groups 1° and 2° (mixed atom types).[42] The following AA residues were considered as hydrophobic in this communication: Ala, Cys, Ile, Leu, Met, Phe, Trp, and Val. The sums of interatomic distances for each AA residue were placed on triangular maps that have AA sequences as coordinates. The integral numbers that make up different clusters correspond to the following: 1° interactions within particular secondary structure; 2° interactions between two or more structured segments; 3° a complex network of interactions taking place between diverse structural elements including a single AA residue. A compact interaction cluster is being formed when the integers are contained in the nearby sequence positions in the triangular distance map, whereas the integers are positioned within $i \leq i + 3$ AA sequence positions in a loose interaction cluster. The numbers of interactions were normalized in the presentations of some graphics. We used the bulkiness value of Gly residue as reference.[43] The bulkiness values of the AA residues were divided by the bulkiness of Gly, and thus an established scale was used for the normalization of the number of interactions per AA residue that is given by eq 2,

$$\mathrm{NI}_i(\mathrm{norm}) = \mathrm{NI}_i/(\text{bulkiness of Gly})/(\text{bulkiness of given AA}) \tag{2}$$

where NI_i is the number of the distances ≤4.5 Å between residue i and the other AA residues. Debye–Waller (B) factors were normalized using the following transformation (3),

$$B_{\mathrm{norm}} = \{(B(j) - \mathrm{ave})2/\sigma\} \tag{3}$$

where ave is the average B-factor and σ is its standard deviation. In the majority of cases, the normalized B factors were not higher than 10. The short stretches of the N- and C-terminal residues were not included in the normalization process.

Force Field Used and Energy Computing. Only the van der Waals (vdW) and Coulombic (elec) terms were used in the calculation of the energy diagrams using the AMBER protein force field.[44] The Lennard-Jones potential function was used.[45] The sum of the vdW and elec energy terms for each AA residue was multiplied by 0.5 since the interaction energy is due to different combinations of atoms in AA residues i and j. Pairwise differential interaction energy patterns for a given pair of chosen 3D structures were calculated from the corresponding aligned sequences. This allowed for an estimation of overall differences in the vdW and elec terms for each AA residue that are due to some fine changes of the compared structures.

Software Availability. All the programs used in this work were written in Fortran 77 by the author and were executed on a Powerbook G4 (Macintosh) and a desktop PC (Hewelett-Packard). The programs were compiled using the Absoft Fortran compiler (version 9.0; Absoft Development Tools and Language, Rochester Hills, MI) for the Macintosh and PC series of computers. The programs used for formation of the 2D distance maps from crystallographic structures and information entropy graphs

Table 1. Molecular and Functional Features of the Major Forms of the FKBPs Expressed in Human Cells[a]

no	protein	FKBD(s)[b] Figure 1A	sequence traits of the FKBDs pI[c]	HI[c]	Ac[d]	triad(s)[e]	major associated entities	cellular/systemic functions
					I FKBP12s			
1	hFKBP12a[6,7]	1 (1)	8.9	25.2	W	AYG	FK506/Calcineurin(A + B)[46,47]	control of T-cell gene transcription (immunosuppression)[1]
							Rpm/FRAP[48,50]	control of T-cell receptor signalization pathways
							type I TGFβ receptor[51,52]	
							muscle ryanodine receptor[53]	
							Inositol receptor[54]	
2	hFKBP12b	1 (2)	8.8	29.6	F	AYG	cardiac ryanodine receptor[53]	
3	hFKBP12c	1 (3)	8.6	25.0	W	AYG		
					II ER-specific FKBPs			
4	hFKBP15p	1 (4)	9.4	25.6	W	GYG		protein folding cofactors[55]
5	hFKBP22p	1 (5)	5.1	48.7	L	AYG		
6	hFKBP25p	1 (6)	7.2	27.8	L	AYG		
7	hFKBP24p	1 (7)	9.2	36.7	W	GYG		
8	hFKBP63p	4 (8–11)	4.8	39.5	M	AYG, AYG, GYG, GYG		
9	hFKBP65p	4 (12–15)	5.8	45.1	M	GYG, AYG, AYG, AHG		
					III TPR motifs containing FKBPs			
10	hFKBP36[56]	1 (16)	4.8	50.9	M	AYG		Williams syndrome,[57]male fertility[26] homologous chromosome pairing in meiosis[26]
11	hFKBP37[58,60]	1	6.1	35.1			aryl receptor[59]	transcription of genes[58,60]
12	hFKBP37i[24]	1	5.7	43.3				Amaurosis syndrome[24]
13	hFKBP38[61]	1 (21)			L	CYG	Bcl[62,63]	development of cancer cells[25,64] sonic hedgehog signaling[65]
14	hFKBP51[66,67]	2 (17) I	8.2	38.3	W	AYG	steroid receptor	Rett syndrome,[6]depressive episodes[69]
		(18) II	4.9	22.2	I			
15	hFKBP52[70]	2 (19) I	4.7	40.0	W	AYG	steroid receptor[71]	Refsum syndrome[72]control of Ca^{2+} channels[73]
		(20) II	5.0	12.1	L	AFG		
					IV other FKBPs			
16	hFKBP25n[8,81]	1 (23)	9.9	16.5	W	AYG	YY1[74]HMG-II[75,76]	transcription of genes
17	hFKBP135	1 (22)	5.7	52.5	W	AVG	F-Actin[5]	colocalized with F-Actin; the growth cones of dorsal root ganglion neurons[5]

[a] Only some major targets of the FKBPs and their cellular functions published to date were cited. [b] The numbers in the third column correspond to the FKBD repeats in a given FKBP. In parentheses are the indexes corresponding to the sequences in Figure 1A. [c] The pIs and HIs were calculated for the FKBDs only and not the entire FKBP sequence. [d] Central AA residue in the PPIase cavity. [e] AA-residue hallmark in the 80s loop.

calculated from the MSAs can be obtained upon request. 2D maps decorated with different elements were made with the ClarisDraw program.

RESULTS

Gradient Maps of the AA Substitutions in the FKBPs. The genomes of different organisms may encode from none to several dozens of diverse paralogues of the 12 kDa archetypal FKBP.[2] In the human genome are encoded at least seventeen proteins consisting from one to four FKBDs and diverse sequence motifs.[2,29] Several other ORFs and pseudogenes encode FKBD-like sequences whose biological significance remains unknown.[9,10] In Table 1 are summarized diverse data on the paralogues of the FKBPs expressed in human cells, whereas in Figure 1A is shown an alignment of the FKBDs from human FKBPs, with the exception of hFKBP37[58–60] and its variant encoded on human chromosome XVII[24] that have one TPR motif inserted in their FKBDs. In the lower panel of Figure 1A are shown the unique sequences of the FKBDs from diverse organisms whose structures were deposited in the PDB.[38] Vertical color bars indicate the conserved cysteine residue (deep yellow), the innermost AA residue in the PPIase cavity (salmon), and the −AYG− triad and its sequence variants (violet) that is a hallmark of the FKBDs. In Figure 1B is shown a PyMol[77] model of the archetypal hFKBP12a with its typical arrangement of the secondary structure.[78,79] In Figure 1A, β-strands are indicated as horizontal blue bars and β-turns are in green, whereas α- and G-helices are in light yellow. The archetypal hFKBP12a has a high sequence similarity to its two isoforms hFKBP12b and c, whereas the sequence similarity scores (IDs) between the hFKBP12a and its remaining human paralogues are in low ranges (see Figure 1A), which show for a considerable diversification of their sequences.[30]

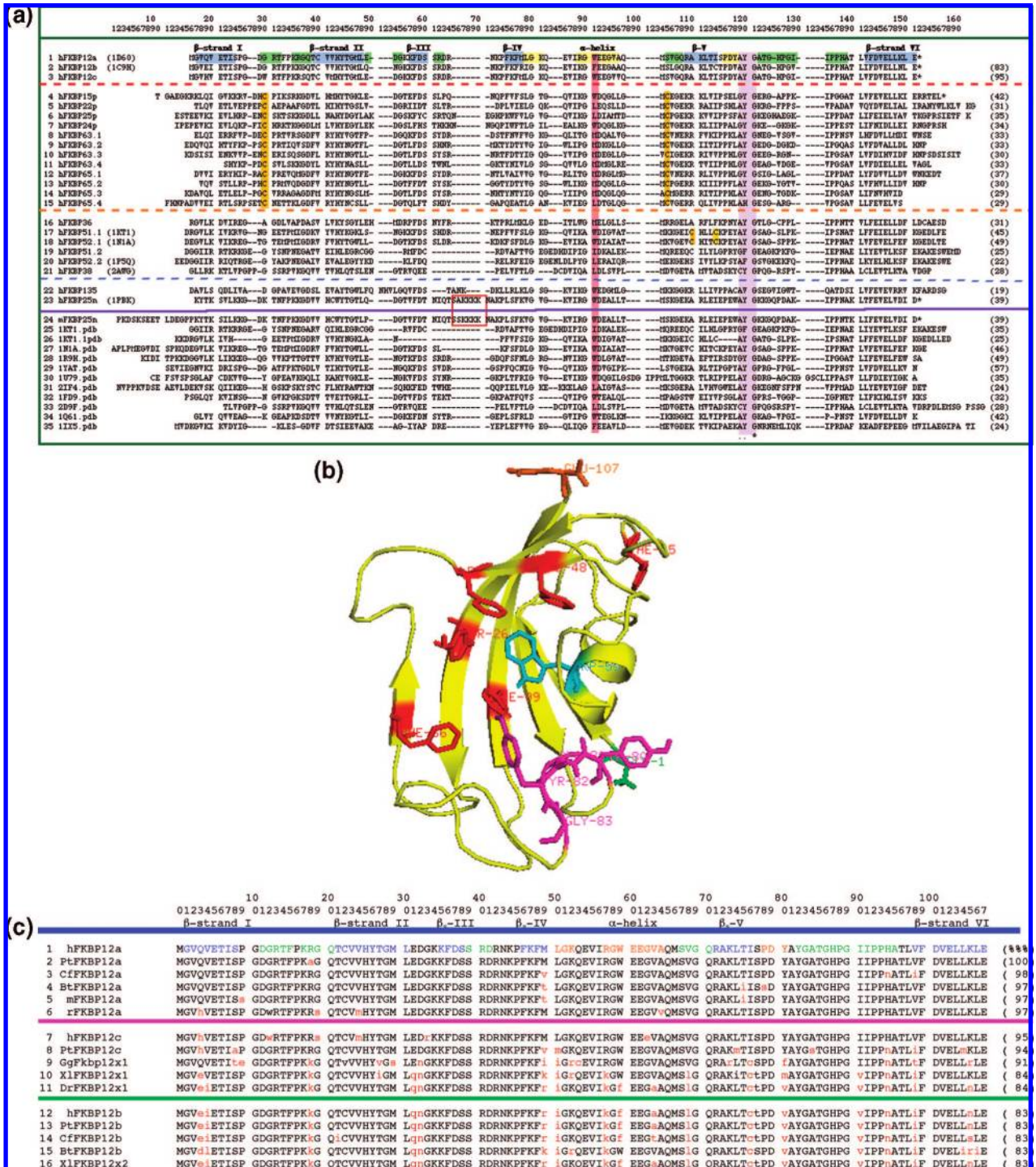

Figure 1. A. MSA of the human FKBDs and the unique sequences extracted from the X-ray structures of the FKBPs.[38] The PDB codes and sequence similarity scores (ID, %) to the top sequence (the archetypal hFKBP12a) are given at the right side of the figure. The aligned sequences are as follows: (1–3) small FKBPs, hFKBP12a (NP_463460), hFKBP12b (NP_004107), hFKBP12c (Hs_7697_26_5_1); (4–15) ER-specific FKBPs, namely (4) hFKBP15p (NP_476433), (5) hFKBP22p (NP_057678), (6) hFKBP25p (NP_851939), (7) hFKBP24p (NP_060416), (8–11) the four consecutive FKBDs from hFKBP63p (NP_009201), (12–15) the four consecutive FKBDs from hFKBP65p.

Figure 1 continued. Each of the FKBDs in mammalian ER-residential FKBPs (4–15) have two invariable Cys residues;[80] (16) hFKBP36 (AAC64249); (17 and 18) FKBDs-I from hFKBP51 (NP_004108) and hFKBP52 (NP_002005); (19 and 20) the FKBDs-II from hFKBP51 and hFKBP52; (21) the FKBD from hFKBP38 (NP_036313); (22) the FKBD from hFKBP135 (AB014575); (23) the C-terminal FKBD from hFKBP25n (NP_002004), which has a unique Lys-rich insert (red square) between a G-helical turn and β-strand IV;[82] (24) the FKBD from mFKBP25n;[129] (25 and 26) the two consecutive FKBDs from the X-ray structure (1KT1) of FKBP51 from *Saimiri boliviensis*;[97] (27) 1N1A, the N-terminal domain of hFKBP52;[98] (28) 1R9H, FKBP from *C.elegans*;[99] (29) 1YAT, FKBP12 from *S.cerevisiae*;[89] (30) 1U79 ER-specific FKBP from *A.thaliana*;[55] (31) 2IF4, FKBP42 from *A.thaliana*;[101] (32) 1FD9 FKBP25 *Legionella pneumophila*;[103] (33) 2AGW, the FKBD from hFKBP38;[96] (34) 1Q61, a truncated form of the FKBP from *E.coli*;[104] (35) 1LX5, NMR structure of an FKBP from *Methanococcus thermolithotrophicus*.[105] (B) PyMol model of hFKBP12a (1D60) with the explicitly shown network of aromatic AA residues. (C) Gradient map of the AA substitutions in the small FKBPs using the sequence of hFKBP12a as reference. The AA substitutions with respect to hFKBP12a were explicitly written in small red letters. In parentheses are given the IDs between hFKBP12a and the small FKBPs as listed below: 1 hFKBP12a (A35780); 2 PtFKBP12a (ChimpFk1a); 3 CfFKBP12a (DogFk1a); 4 BtFKBP12a (A61431); 5 mFKBP12a (JH0528); 6 rFKBP12a (U09386); 7 hFKBP12c (Hs6_7697_26_5_1); 8 PtFKBP12c (ChimpFk1c); 9 GgFKBP12x1 (NF00049319); 10 XlFKBP12x1 (JC5764); 11 DrFKBP12x1 (NP_957106); 12 hFKBP12b (JC2188); 13 PtFKBP12b (ChimpFk1b); 14 CfFKBP12b (DogFk1b); 15 BtFKBP12b (A53924); 16 XlFKBP12x2 (AAH41748); 17 mFKBP12b (NP_058559); 18 rFKBP12b (FKBB_RAT); 19 XlFKBP12x3 (AAH61673); 20 DrFKBP12x2 (NP_0010055); 21 XlFKBP12 (NF01923332); 22 TnFKBP12 (OdonFk1b); 23 GgFKBP12x2 (BAB89371); 24 DrFKBP12x3 (AAH59682); 25 TnFKBP12x1 (OdonFk1a); 26 SdFKBP12 (Q966Y4); 27 TrFKBP12 (FuguFk1a); 28 DmFKBP12x1 (F57582.1); 29 DmFKBP12x2 (S54139); 30 MsFKBP12 (AAF16717); 31 AgFKBP12 (EAA00155); 32 CiFKBP12 (CAC82550); 33 CeFKBP12 (U27353); 34 SpFKBP12 (AL021816); h [*Homo sapiens*]; Bt [*Bos taurus*]; Cf [*Canis familiariz*]; m [*Mus musculus*]; r [*Rattus norvegicus*]; Pt [*Pan troglodytes*]; Gg [*Gallus gallus*]; Xl [*Xenopus laevis*]; Dr [*Danio rerio*]; Tn [*Tetraodon nigroviridis*]; Sd [*Suberitis domuncula*, (Sponge)]; Tr [*Takifugu rubripes*]; Dm [*Drosophila melanogaster*]; Ms [*Manduca sexta*]; Ag [*Anopheles gambiae* str. *PEST*]; Ci [*Ciona intestinalis*]; Ce [*Caenorhabditis elegans*]; Sp [*Schizosaccharomyces pombe*].

Analyses of the small MSA shown in Figure 1A and several large MSAs consisting from 300 to 499 sequences of diverse FKBPs and FKBDs revealed that the major deletion/insertion (indels) took place in the sequence patches flanking β-strand III. The Pola_SQ clustering algorithm[29] used the MSA of 487 FKBDs (see Supporting Information Appendicies 1.1 and 1.2) and several attributes that are typical for the differentiated sequences of the FKBDs and sorted them into functionally coherent groups of proteins. For example, using the sequence of hFKBP12a as a template, the algorithm extracted from the MSA the close orthologues of the protein which are shown above the pink line in Figure 1C; in the parentheses are given the IDs while small red letters indicate the AA substitutions with respect to the sequence of hFKBP12a. Below the pink line, are shown several orthologues of hFKBP12c that are followed by the orthologues of hFKBP12b and diverse small FKBPs encoded in different genomes. The numbers of small FKBPs encoded in different genomes vary from seven in *A.thaliana*,[29] four in diverse genomes of fishes,[83] to three in genomes of different mammals.[2] Some short patches of the sequences are highly conserved, namely the N-terminal AA triad of the central α-helix is well conserved in the orthologues of hFKBP12a (−RGW−), in the orthologues of hFKBP12b usually it is −KGF−, whereas the −KGW− triad is often found in prokaryotic FKBP12s.

The FKBD from the ER-specific hFKBP25p used as a template clustered with its orthologues from diverse genomes and with a series of the orthologues of the ER-specific hFKBP24p. The FKBDs from large hFKBP65p and hFKBP63p had a tendency to cluster together with the small archetypal ER-specific hFKBP15p. The FKBDs-I and -II from hFKBP51 and hFKBP52 clustered with its orthologues encoded in different genomes. The FKBDs from hFKBP36, hFKBP37, hFKBP38, hFKBP25n, and hFKBP135 were clustered only with their proper orthologues encoded in various genomes because they possess some fine sequence traits (see Table 1) that are different as those in the four groups of the sequences described above, namely 1° FKBP12a + FKBP12b + FKBP12c have similar pIs and HIs; 2° FKBP24p + FKBP25p have similar pIs, HIs, and AACs; 3° the FKBDs-I in FKBP51s and FKBP52s are hydrophobic whereas the FKBDs-II are hydrophilic; and 4 °FKBP63p + FKBP65p which have four FKBDs with very similar pIs and HIs; FKBP15p clustered with them since it has a similar HI.

Conservation of the Sequence Traits in the FKBDs. Analyses of the sequence conservation of the PPIase activity site and diverse sequence hallmarks of the FKBDs are shown in Table AT1 (Supporting Information Appendix 1.3). The levels of conservation within the PPIase cavity in the large MSA containing 487 diverse FKBDs (see Supporting Information Appendix 1.2) are similar to those calculated for the seventeen unique sequences extracted from the X-ray structures of the FKBPs. We tentatively assumed that the sequences of diverse FKBDs consist quasi-similar distributions of the secondary structures as those that had been established from the X-ray structure of hFKBP12a.[78,79] The sequence stretches of the secondary structures have moderate levels of conservation (see Table AT1). High conservation levels display some Gly residues and the aromatic/hydrophobic AA residues that are close to the PPIase cavity, and the network of interacting aromatic/hydrophobic AA residues that are probably crucial for the structural stability of the FKBDs. Several other sequence positions of hFKBP12a projected onto the entire MSA containing 487 sequences of diverse FKBDs remain highly conserved, namely V2, H25, G51, M66, G69, K73, Y82, G83, G86, G89, P92, P93, T96, and F99. An exceptionally high conservation was noted for the triad −AYG− (hFKBP12a) and its sequence variants, such as −GFG−, −AFG−, −GYG−, −AHG−, or −CYG− (see Table 1), that are in the long loop linking β-strands V and VI that are often called the "80s loop". The triad is often preceded by an aromatic AA residue or a bulky AA residue (L, K, or V). Information entropy (Ie) graphs for 487 sequences (pink bars) of the FKBDs and 17 unique sequences (green bars) of diverse FKBDs extracted from the PDB files (see Table 2) are shown in Figure 2. In general, the Ie values are higher in the MSA of 487 FKBDs with few exceptions due to an under-representation of certain types of the FKBDs in the set of the crystallographic data.

3D Structures of the FKBDs. Table 2 contains the results of some basic analyses of the 3D structures of the FKBPs whereas in Figure 1B and Figure 1AD−AG (Supporting Information Appendix 1.4) are shown the PyMol models of the FKBDs with the explicitly shown aromatic AA residues (in red), W59 (hFKBP12a) and its spatial equivalents in the

Table 2. Crystal Structures of the FKBDs from Diverse Organisms

no	protein/Ligand	PDB	length	res (Å)	NID	AAs with high Bs	ref
1	hFKBP12a	1D6O	107	1.85	2093	38EDGKK, 41DRN	84
2	hFKBP12a	1FKJ	107	1.70	2054	17KPGQ	88
3	bFKBP12a	1FKK	107	2.20	2250	41DRNK, 83GA, 99F	88
4	hFKBP12a/FK506	1FKF	107	1.70	2113	17KRGQ, 42RN, 89G	78, 79
5	hFKBP12b/Rpm	1C9H	107	2.00	2137	19GD, 41DRNK, 49RIG	85
6	hFKBP12a/Rpm	1FKB	107	1.70	2112	32DG, 41D, 43NK, 88P	78, 79
7	bFKBP12a/Rpm	1FKL	107	1.70	2112	18R, 32D, 40RDRNK	88
8	hFKBP12a/Lig1[a]	1FKH	107	1.95	2173	44K, 84A, 87HPGI	17
9	hFKBP12a/Lig2[b]	1FKI	107	2.20	2126	32D, 41DRD, 88PG	17
10	hFKBP12a/Lig3[c]	1D7J	107	1.85	2113	31EDGK, 41DRN	84
11	hFKBP12/L-709,858[f]	1QPF	107	2.50	1980	12G, 18R, 32D, 52K, 54E, 83G, 89GI	95
12	hFKBP12/L-685,818[e]	2FKE	107	1.72	2109	17KRGQ, 41DRN	89
13	hFKBP12/L-707,587[g]	1QPL	107	2.90	1934	33GK, 83GAT	89
14	hFKBP12/FK506/CnA/CnB	1TCO	107	2.50	2272	26YT, 35KDSS, 41DR, 84A	90
15	hFKBP12/Rpm/(FRAP)	1NSG	107	2.20	2000	13R, 16PKRG, 51GK	91
16	hFKBP12/Lig4[d]/(FRAP)	2FAP	107	2.20	2078	13R, 17KR, 52K	92
17	hFKBP12a/(TGFβ-R type I)	1B6C	107	2.60	2206	18R, 31EDGK	93
18	hFKBP12a (R42K/H87V)	1BKF	107	1.60	2103	18RG, 39SRDKNK	86
19	hFKBP12a (F36V)	1BL4	107	1.90	1998	31ED, 85TGHPGI	87
20	hFKBP12a	2DG3	107	1.70	2103	39SRDRNK	94
21	hFKBK12a/Rpm (W59F)	2DG4	107	1.70	2003	31EDG, 38SSRDRNK	94
22	hFKBP12a/Rpm (W59L)	2DG9	107	1.70	2036	31EDGK, 40RDRN	94
23	hFKBP12a/FKB-001	1J4R	107	1.80	2245	19G, 31EDG, 51GKQE	18
24	hFKBP25 (C-terminal)	1PBK	116	2.50	2262	150NTSAKKKKNA	82
25	hFKBP38	2AWG	118	1.60	2140	91EE, 113G, 132ENG	96
26	hFKBP51	1KT1	374	2.70	7588	42HGE, 56HYNGKLAN, 76PFV 107C, 126ATL, 131E	97
27	hFKBP52 (N-terminal)	1N1A	121	2.40	2257	16APLPM, 43GT	98
28	hFKBP52 (C-terminal)	1P5Q	283	2.80	6691	179K, 181KL, 303E, 424KAKA	98
29	CeFKBP12 (F31D4.3)	1R9H	118	1.80	2310	25QG, 56RGD, 66R	99
30	AtFKBP13	1U79	129	1.85	2429	101SDRG	55
31	AtFKBP13 (Reduced form)	1Y0O	129	1.89	2393	none	
32	AtFKBP42 (N-terminal)	2F4E	131	2.32	2577	80NSQ	100
33	AtFKBP42	2IF4	258	2.85	5949	165KARS, 192E, 279QMDSAR, 290AQ	101
34	ScFKBP12	1YAT	113	2.50	2164	11DGAT, 31NQG	102
35	LpFKBP25	1FD9	204	2.41	2140	none	103
36	EcFKBP29 (MIP-like)	1Q6H	210	1.97	4340	23S, 29A, 34Y, 36(M-Se), 42N, 51KD, 57GV, 98(M-Se), 131GEAP, 153GKED	104
37	EcFKBP29/FK506	1Q6I	210	2.25	4273	22KSA, 34Y(M-Se)E, 63A, 110F, 134ED	104
38	EcFKBP29/Rpm	1Q6U	213	2.45	4295	132KGE, 154KEFDNSYTRGE, 171DG	104
39	MtFKBP17	1IX5	151				105

[a] Lig1 = (1*R*)-1-cyclohexyl-3-phenyl-1-propyl (2*S*)-1-(3,3-dimethyl-1,2-dioxopentyl)-2-piperidinecarboxylate. [b] Lig2 = (21*S*)-1-aza-4,4-dimethyl-6,19-dioxa-2,3,7,20-tetraoxobicyclo19.4.0pentacosane. [c] Lig3 = 4-hydroxy-2-butanone. [d] Lig4 = C16-ethoxy rapamycin. [e] L-685,818 = 18-hydroxyascomycin. [f] L-709,858 = C32-*O*-(1-ethyl-indol-5-yl)-ascomycin. [g] L-709,587 = C32-*O*-(1-methylindol-5-yl)-18-hydroxy-ascomycin.

other FKBDs (in cyan), and the −AYG− triad and its sequence variants (in rose). The N- and C-terminal AA residues in given FKBD were colored in green and orange, respectively. The numbers of interatomic distances (NID) within 2.7–4.5 Å are similar for the diverse FKBDs (see Table 2). The NID factor is a sum of diverse intramolecular interactions which in the structure of hFKBP12a (1D60) have the following distributions (distances ≤ 4.5 Å): (I) 29% of the interactions are between the hydrophobic atoms, 19% between the hydrophilic atoms, and 52% for mixed types; (II) 40% of the interactions are between the main chain atoms, 34% between the main chain/side chain atoms, and 26% between diverse side chain/side chain atoms. Similar distributions of atomic interactions were obtained for the other structures of the FKBDs. In Figures 3A and B and 3CA are shown three bidimensional (2D) distance maps (distances ≤ 4.5 Å) calculated from the following pairs of structures, namely (A) the archetypal hFKBP12a (1D60, upper triangle) and its close paralogue hFKBP12b (1C9H, lower triangle); (B) the C-terminal FKBD from human nuclear FKBP25; and (C) the FKBD from hFKBP38. For comparison at the lower triangles of B and C is shown the

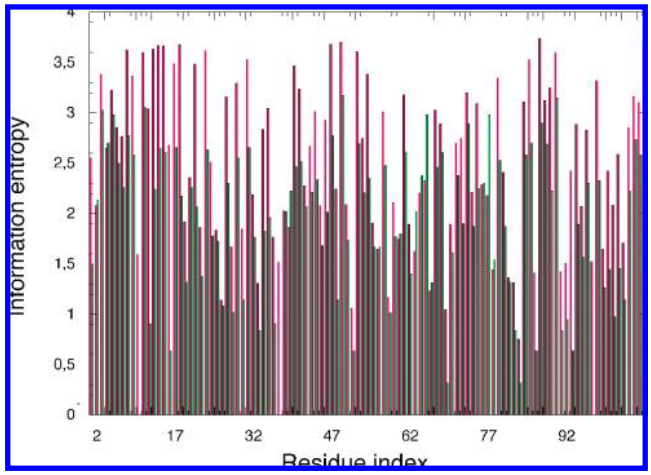

Figure 2. Information entropy (Ie) calculated from the MSAs of 487 FKBDs (red bars) and 17 unique sequences of the FKBDs extracted from the PDB files (green bars).

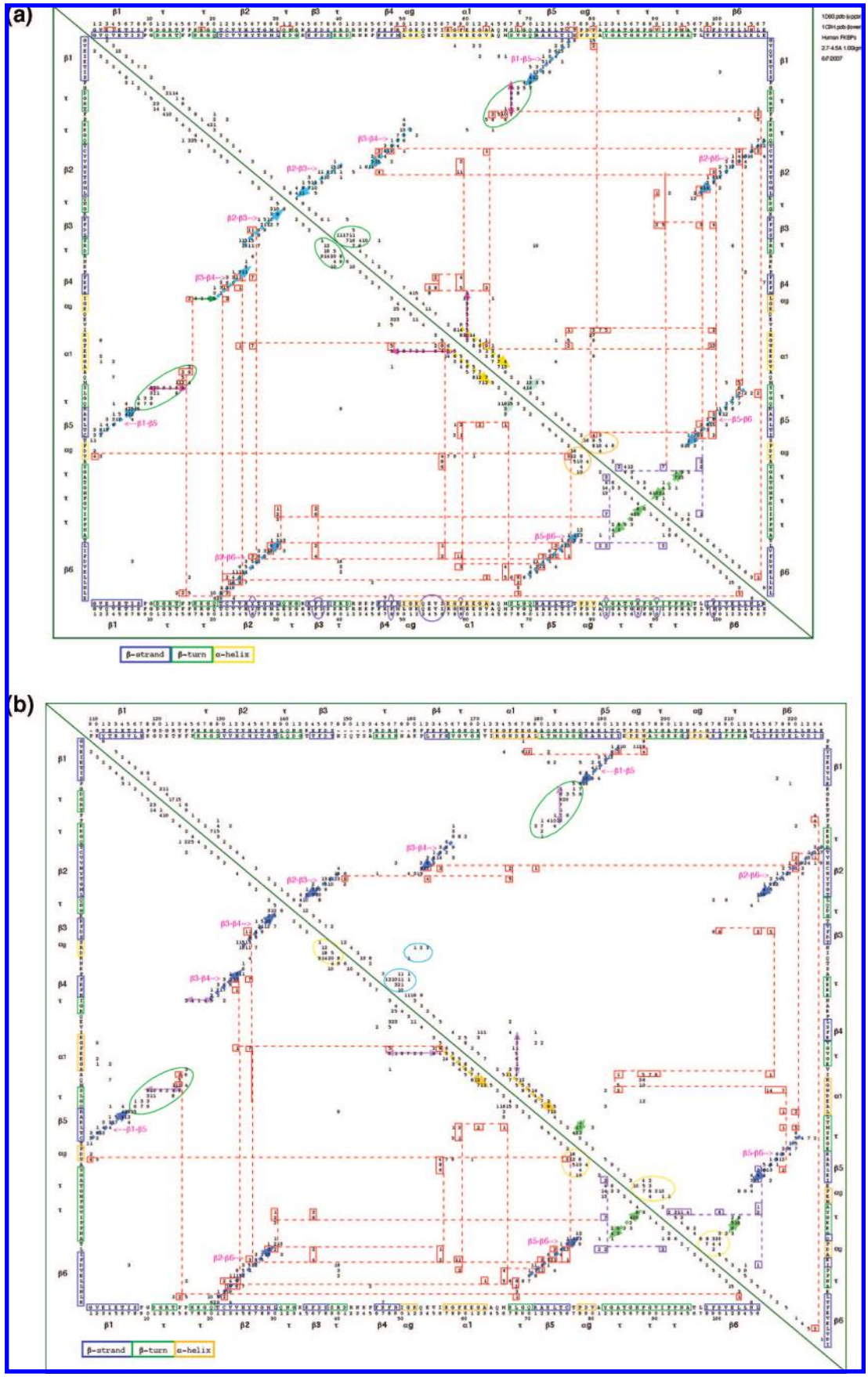

Figure 3. Two-dimensional maps of intramolecular atomic interactions shown explicitly as the integer numbers in the following pairs of structures: (A) 1D60 (hFKBP12a, upper triangle) and 1C9H (hFKBP12b, lower triangle); (B) 1PBK (FKBD from hFKBP25, upper triangle)[82] and 1C9H (hFKBP12b, lower triangle).

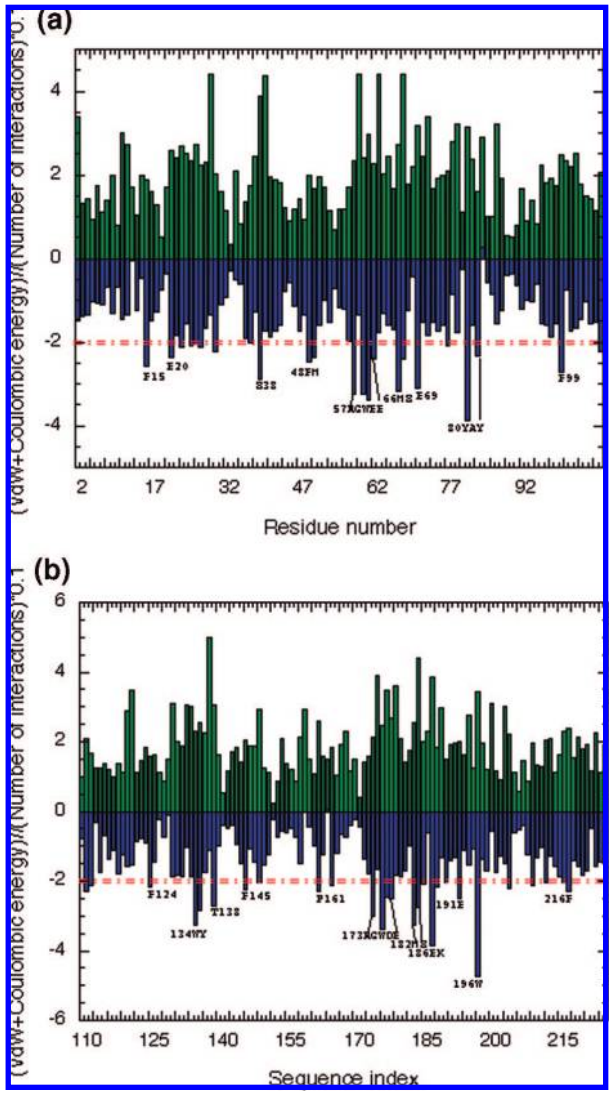

Figure 4. Numbers of interactions (green bars) and the sum of the vdW and Coulombic energy terms (blue bars) per each AA residue for (A) 1D60 (upper panel) and (B) the FKBD from hFKBP25n (1PBK, lower panel) with the explicitly written patches of sequences that are crucial for PPIase activity and the aromatic AA residues. The red dashed double lines at the bottom parts of both figures were arbitrary placed at a −2.0 kcal/mol level.

interatomic distance map for hFKBP12b (1C9H) (Figure 3CA is in Supporting Information Appendix 1). The clusters of the integers corresponding to β-structures are indicated as blue arrows, whereas α-helices are positioned close to the diagonal of the 2D map and are shown as yellow arrows. The clusters of atomic distances within some β-turns are shown as green ellipses or green fat double-edge arrows, whereas the distances within the AA residues in G-helices are shown as yellow ellipses. The violet ellipses on the sequence (horizontal axes) were placed on the AA residues that are crucial for the binding of FK506 and PPIase cavity. Distributions of the main interaction clusters on the 2D maps derived from these four FKBDs are similar despite the moderate IDs of their respective sequences, namely hFKBP-12b/hFKBP25n (ID = 39%) and hFKBP12b/hFKBP38 (ID = 25%). The interaction networks of the hydrophobic AA residues surrounding the PPIase cavity however were altered to different degrees in these four FKBDs.

Analyses of the AA substitutions derived from the MSAs, the 2D interatomic distance maps, and the 3D structures of the FKBDs revealed that fine features of their macrolide-binding sites were altered to different levels. These changes are due to some modifications of the secondary structure elements and the networks of the hydrophobic AA residues surrounding the macrolide-binding cavity. In the four structures (1D6O, 1C9H, 1PBK, and 2AWG), the main clusters of interactions and the interaction networks of the hydrophobic AA residues are centered on β-strands II, V, and α-helix. Moreover, at least three distinct linear clusters of distances, indicated as constant double-edge arrows, are well-conserved in all these four structures. The pink arrow indicates the interactions of Glu60 that cover the five nearby AA residues (hFKBP12a and b). It corresponds to a similar linear cluster for Asp100 and Asp176 in the FKBDs of hFKBP38 and hFKBP25, respectively. Ile50 (hFKBP12b), Leu50 (hFKBP12a), and Ser67 (both FKBP12s) have similar distributions of linear clusters (see light violet arrows).

Intramolecular Interaction Networks in the FKBDs. Analyses of the overall hydrophobicity (HI) of diverse FKBDs revealed that the FKBDs-II of hFKBP52 and hFKBP51 are hydrophilic and hFKBP12a and the FKBD of hFKBP25n have a moderate hydrophobicity, whereas the FKBDs of hFKBP135, hFKBP38, and hFKBP36 and in those of the diverse ER-specific FKBPs are highly hydrophobic (see Table 1). The hydrophobic AA residues interaction networks in the FKBDs were marked down in red squares and dashed lines (see Figures 3A and B and 3CA). The majority of the interaction clusters formed by the hydrophobic AA-residues are positioned around the PPIase activity cavity. The interaction network of the highly conserved −AYG− triad was marked down in violet. It is connected to the interaction network of the hydrophobic AA-residues that surround the PPIase activity site. These two interaction networks are extensive in the structures of the small FKBP12s and involve in a particular fashion the central α-helix and β-strands II and V (Figure 3CA). In Figure 3B are shown the interatomic distance maps for the FKBD in hFKBP25n (1PBK, upper panel) and for comparison the distance map for hFKBP12b (1C9H). In Figure 4A and B are shown linear representations of the upper triangles of Figure 3A and B with the sum of Coulombic and vdW energy terms calculated for distances in the range 2.7 Å ≥ d ≤ 4.5 Å. The interaction network of the hydrophobic AA residues is more extensive in hFKBP12b than that in the FKBD of hFKBP25. The interaction networks involving the −AYG− triad (violet squares) are well conserved in both structures, although a Trp residue (W196 in hFKBP25n) is in the place of Y80 (hFKBP12a) which makes that it is the most intense interaction site in the FKBD of hFKBP25n (see Figure 4B). In both cases, the interactions between Y198 and F216 (hFKBP25n) and Y82 with F99 in hFKBP12b (see Figures 3B and 4A) are conserved. In Figure 3CA is shown 2D maps of interatomic distances in the FKBD from the hydrophobic FKBP38 (upper panel) and for comparison that of hFKBP12b (1C9H). There is about 28% sequence similarity between these two FKBDs while the K_d of Rpm binding to hFKBP38 is about 500 nM[106] as compared to 0.4 nM for hFKBP12a. The PPIase activity site is not as richly surrounded with the aromatic AA residues as it is the case in the FKBDs of hFKBP12a and hFKBP25n.

Intramolecular Interaction Networks in the Free and

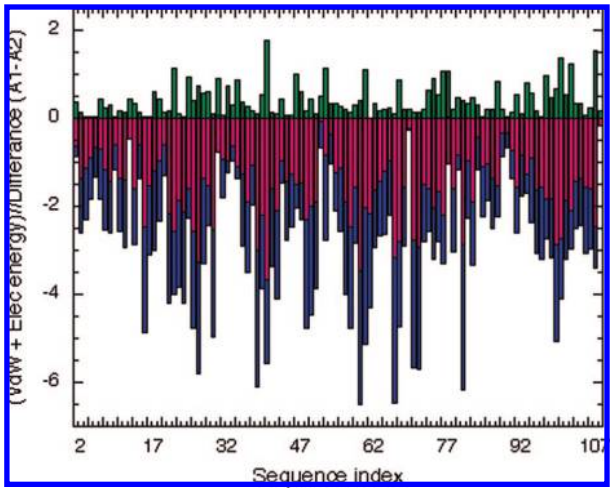

Figure 5. Differences in vdW and Coulombic terms in the couples of structures: hFKBP12a (1D60, blue bars) and FK506 bound to hFKBP12a (1FKB, red bars).

Bound Forms of hFKBP12a. It has been suggested that there is an insignificant change of the structure of hFKBP12a after its binding to FK506[107] which would imply that the structure of the small FKBP is rigid and no particular adjustment of the protein to the hydrophobic macrolide took place. NMR studies have revealed however, that overall flexibility of the loop linking β-strands V and VI decreased upon binding FK506 to hFKBP12a.[108] An overall root-mean-squared deviation (rmsd) calculated for the CA atoms of 1D6O and 1FKB is 0.6016, which is somewhat smaller than the rmsd between the CA atoms in the free form of hFKBP12a (1D6O) and the hFKBP12b/Rpm complex (1C9H), namely rmsd = 0.7236.

In Figure 5 is shown a difference graph (upper panel) derived from the 2D maps of the intramolecular interactions in a free form of hFKBP12a (1D60, red bars) and in its complex with FK506 (1FKB, blue bars); the bars were superimposed onto each other (lower panel). The graphs show that only some insignificant changes took place in the vdW and Coulombic interactions between the AA residues in $i \geq (i + 2)$ sequence positions and at distances ≤ 4.5 Å.

Intermolecular Interaction Networks between the FKBDs and Their Targets. FKBPs interact with different proteins either via their FKBDs or the other sequence motifs such as TPRs, TMs, CBD, etc. Several structures shown in Table 2 represent binary and ternary complexes of the FKBPs with diverse ligands. Crystal structure of the kinase domain of TGFβ-RI bound to hFKBP12a (1B6C)[93] revealed that 260 interactions below 4.5 Å are formed between the two components of the complex. The following AA residues are involved in the FKBP: Y26, F36, D37, D41, R42, F46, K47, Q53, E54, V55, I56, W59, Y82, T85, H87, P88, G89, I90, F99. These AA residues belong to the PPIase cavity and the loop linking β-strands V and VI, which implies that the entire binding groove of hFKBP12a was filled up by several AA residues from the kinase domain, namely hydrophobic L195, L196, V197, charged R199, and hydrophilic P194, T200, T204. The loop linking β-strands V and VI (80s loop) interacts with several AA residues of the kinase domain, namely W242, F243, A246, E247, Q250, T251. The rmsd calculated for the 10 CA atoms (AAs 80–89, 1D60) and its bound counterpart to the kinase domain (1B6C) is 0.441 with the greatest displacements for G86 and P88. These residues have high conservation and low Ie values (see the MSA, Supporting Information Appendix 1.2).

The FKBP12a/FK506 binds to calcineurin/calmodulin[46,47,109] whereas FKBP12a/Rpm interacts with TOR1 (yeast cells)[48] and with the kinase FRAP (mammalian cells).[49,50] The following numbers of interactions below 4.5 Å take place in the ternary complex (1TCO)[109] bFKBP12a/FK506 (calcineurin's subunits A, B and calmodulin): (1) 175 between the atoms of FK506 and FKBP12a; (2) 121 between hFKBP12a and calcineurin A; (3) 99 between hFKBP12a and calcineurin B; (4) 79 between calcineurin A and FK506; (5) 19 between FK506 and calcineurin B; and (6) 461 between calcineurin A and B subunits. The ternary complex hFKBP12a/Rpm/FRAP has (1) 125 interactions below 4.5 Å between rapamycin and the FRAP protein, (2) 173 interactions between rapamycin and hFKBP12a, and (3) 83 interactions between hFKBP12a and the kinase domain that involve the following AA residues in the FKBP: T21, F36, R42, F46, K47, F48, E54, Y82, T85, G86, H87, P88, P89, I90.

The above analyses show that the AA residues from the long loop linking β-strands V and VI positioned at the bottom of the models shown in Figure 1B and Figure 1AD−AG (Supporting Information Appendix 1.4), have multiple contacts in complexes with diverse proteins. Analyses of the conservation of the sequence positions in the FKBDs from diverse species revealed that one of the highest conservation levels and the smallest Ie has the Gly residue in the −AYG− triad and its sequence variants (see Table 1). G81 in the −AYG− triad (hFKBP12a) has few interactions with the other AA residues at $d \leq 4.5$ Å, and it could be a part of a hinge that facilitates binding of the FKBPs to their targets, while the specificity of the binding would be imposed by the AA residues that flank the Gly residue of the triad. The particular positioning of the triad in the FKBDs (see Figure 1B and Figure 1AD−AF in Appendix 1.4) may imply that it is a crucial recognition site in this family of proteins.

DISCUSION

Gradient maps of the AA substitutions derived from several series of the FKBPs encoded in diverse genomes whose sequences are orthologous to human FKBPs revealed that the substitutions occur, both in the macrolide-binding (PPIase) cavity and in the network of the aromatic/hydrophobic AA residues surrounding it. Although the sequences of human FKBDs are highly differentiated,[2,30] the intramolecular interaction clusters have similar distributions on the 2D-distance maps of the FKBDs from different phyla. Moreover, the rmsds for the CAs of the AA residues that are crucial for PPIase activity remain within 0.5 to 0.7 for different pairwise combinations of the FKBDs. Some groups of the FKBDs retain specific sequence traits, hydrophobicity and pIs which create functional niches for those FKBPs. Such a drift of the sequence attributes in the multiple paralogues of the FKBPs however imposed some subtle diversity within the conserved FKBP-like fold that can be seen on the 2D maps (Figures 3A and B and 3CA) and their linear representations (Figure 4A and B). For example, W59 is in the innermost position of the PPIase cavity of hFKBP12a (see Figure 1A) and is conserved to about 45% in the large MSA. This position may be occupied either by Leu, Ile, Met,

or Phe in the other FKBPs (Table 1). It has been shown that FKBP12a with W59 → F59 and W59 → L59 substitutions bind rapamycin but their thermodynamic stability is somewhat higher than that of the wild type.[94] The structures of these three FKBPs namely, 2DG3 (hFKBP12a, wild-type), 2DG4 (W → F), and 2DG9 (W → L) are very similar. In Figure 3A are indicated all of the 18 AA substitutions in the sequence of hFKBP12a as compared to that of hFKBP12b (see orange squares at the top sequence). These AA substitutions change the binding specificity from a Val-Pro epitope (LSRLVPLDDLV) in a muscle ryanodine receptor (RyR1) that is normally bound to FKBP12a, for a Ile-Pro epitope (LSRLIPLDDLV) in cardiac RyR2 that is normally bound to FKBP12b.[53] The atomic contacts between the macrocycles FK506 or rapamycin and the FKBPs are different than those taking place between the polypeptide chain of the kinase domain of the TGFβ receptor type I (TGFβ-RI) and hFKBP12a. It is thus likely that target specificity of the two small FKBPs is imposed by those 18 AA substitutions, and it is not due only to the identity of the innermost AA residue in the PPIase cavity.

It has been suggested that the ternary complexes (hFKBP12a/FK506)/calcineurin(A + B) and hFKBP12a/Rpm/FRAP[46–50] control crucial signalization pathways in T-cells that would render them inoffensive against transplanted organs. Only about 50% of the hydrophobic surface of the macrolide (FK506 or rapamycin) is hidden in the PPIase cavity of the small FKBPs.[89] This would imply that in vivo a sizable part of the exposed hydrophobic surface of the drug should be hidden in a hydrophobic cavity in order to avoid polar molecules. FKBP12.6 and FKBP51 also bind FK506 and inhibit the phosphatase activity of calcineurin[66,106] and thus in vivo they may sequester it and modulate the overall immunosuppression induced by the drug. The hydrophobic compounds FK506, ascomycin, and rapamycin[14,15,110] should also be sequestered by FKBP25n, FKBP52, and the array of the ER-specific FKBPs. Likewise, the drugs may be trapped by diverse hydrophobic cavities made from the phospholipids and some membrane-embedded proteins.[111] Moreover, it has been shown that FK506 and rapamycin in vivo induce a large spectrum of serious health-threatening effects.[15,16,110] Thus, the subtle spatial diversity in the conserved structure of the FKBDs imposes some specificity in the binding to different small compounds[1,14–16,109–112] but also probably impinge on the binding specificity to diverse epitopes of proteins and other cellular entities (functional drift within the FKBP family of proteins).

The structures of many families of proteins are well conserved,[113] and thus, it is not surprising that the complex hFKBP12a/Rpm binds to mammalian FRAPs while ScFKBP-12/Rpm binds its yeast homologue, TOR1. It has been however reported that rapamycin had no effect of the growth of *A.thaliana* whose genome encodes a homologue of TOR1[114] and an array of the FKBPs.[29] Expression of ScFKBP12 in the plant restored its sensitivity to rapamycin; namely, it reduced the primary root growth and diminished accumulation of large polysomes.[114] It would be interesting however to verify if an endogenous substance bound to FKBP12 could form a complex with the TOR1 or FRAP kinases, and if so, what a functional meaning might it have. This could prove that the ternary complexes hFKBP12a/Rpm/FRAP and ScFKBP12/Rpm/TOR1 mimic functional features

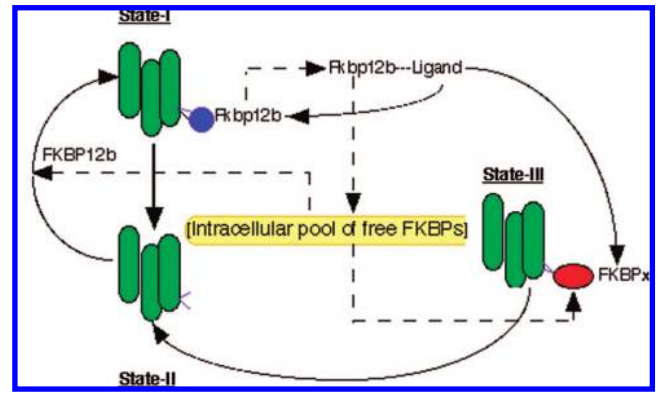

Figure 6. Hypothetical scheme of dynamic exchanges between the FKBPs (small ovals), their small molecular mass ligands, and some large cellular receptors (large green cylinders).

that are not spurious (merely toxic) but that the FKBP12/kinase assembly is under the control of some endogenous factor(s).

Multiple experimental and theoretical studies have been conducted on PPIases activity of FKBP12a[115] and cyclophilin A.[116–121] It has been shown that there is some substrate specificity[122] in PPIase activity exhibited by hFKBP12a and human cyclophilin A, but it also became certain that the inhibition of the activity by FK506 and CsA, respectively, is not related to the immunosuppressive actions induced by these drugs.[1,15] It is due to the fact that a high intracellular concentration of diverse PPIases excludes the possibility of their total inhibition under in vivo conditions.[1,15,110] The binding capacity of the FKBPs and their modulatory effects on the complexes seem to be the principal functional attributes of this family of proteins,[1] whereas PPIase activity itself is their minor functional attribute. It has been shown that small chemical derivatives of FK506 such as V-10,367 or GPI-1046, which lack the effector domain present in the parent compound, increase nerve regeneration in animal models and protect against ischemic shocks.[22,23] It is improbable that the inhibition of PPIase activity of any of the FKBPs would influence nerve regeneration and their protection.[22,23] These effects could be tentatively explained using the following hypothesis that links dynamic competition between diverse ligands of the FKBPs and the functions of some neuronal receptors or ionic channels as depicted in Figure 6. For example, a complex of FKBP12b/small ligand may release the ligand and displace FKBP12b bound to a receptor (state I). This would alter the biological state (function) of the receptor (state II) which may bind to one of the free forms of the FKBPs, e.g., FKBP52, leading to state III or it may return to state I if it binds its preferential ligand, FKBP12b. Such dynamic exchange between the FKBPs, their small molecular mass ligands and large membrane-bound receptors could be responsible for some of the neuroregenerative and neuroprotective actions imposed by FK506 and its small chemical derivatives.[22,23] Experimental data on the interactions between immunophilins and their large membrane protein targets[20–23,53,54] could be addressed using novel theoretical modeling approaches, molecular dynamics simulations,[121,123,124] and computing of free energy of binding.[125,126] Some membrane proteins[127,128] have been investigated with theoretical approaches, thus probably in the future more sophisticated studies could be

carried on modeling of interactions between some immunophilins and their membrane-harbored targets.

Abbreviations. FKBP, FK506 or rapamycin-binding protein; FKBD, FK506-like binding domain; AA, amino acid; PPIase, peptidylprolyl cis/trans isomerase; FK506, an immunosuppressive macrolide; Rpm, rapamycin; TPR, tetratricopeptide repeat; TM, transmembrane segment; CBD, calmodulin binding domain; NLS, nuclear localization signal; ER, endoplasmic reticulum; ID, sequence similarity score; Ie, informational entropy; AAC, amino acid composition; MSA, multiple sequence alignment. Numerical suffixes used to differentiate FKBPs refer to their size in kilodalton.

ACKNOWLEDGMENT

We are indebted to DSV/iBiTec-S/SIMOPRO for financial support. Molecular models were made with PyMOL.[77]

Supporting Information Available: Appendix 1 consisting of the following files: (1.1) seqmsa.out with the data on the aligned sequences; (1.2) fk487.aln which stores the sequence alignment of 487 FKBDs; (1.3) Table A1; (1.4) Figure 1AD−AG; (1.5) Figure 3CA, 2D-distance map derived from 2AGW (the FKBD from hFKBP38, upper triangle)[96] and 1C9H (hFKBP12b, lower triangle).[85]

Appendix 2 consisting of the geometry.out file with the data from the analyses of the following structures: 1D60, 1C9H, 1PBK, and 2AWG. This material is available free of charge via the Internet at http://pubs.acs.org.

REFERENCES AND NOTES

(1) Schreiber, S. L. Chemistry and biology of the immunophilins and their immunosuppressive ligands. *Science* **1991**, *251*, 283–287.
(2) Galat, A. Peptidylprolyl cis/trans isomerases immunophilins: biological diversity-targets-functions. *Curr. Top. Med. Chem.* **2003**, *3*, 1315–1347.
(3) Dornan, J.; Taylor, P.; Walkinshaw, M. D. Structures of immunophilins and their ligand complexes. *Curr. Top. Med. Chem.* **2003**, *3*, 1392–1402.
(4) Leulliot, N.; Vincentini, G.; Jordens, J.; Quevillon-Cheruel, S.; Schiltz, M.; Barford, D. J.; van Tibeurgh, H.; Goris, J. Crystal structure of the PP2A phosphatase activator: implication for its PP2A-specific PPIase activity. *Mol. Cell* **2006**, *23*, 413–424.
(5) Nakajima, O.; Nakamura, F.; Yamashita, N.; Tomita, Y.; Suto, F.; Okada, T.; Iwamatsu, A.; Kondo, E.; Fujisawa, H.; Takei, K.; Goshima, Y. FKBP133: a novel mouse FK506-binding protein homolog alters growth cone morphology. *Biochem. Biophys. Res. Commun.* **2006**, *346*, 140–149.
(6) Harding, M. W.; Galat, A.; Uehling, D. E.; Schreiber, S. L. A receptor for the immunosuppressant FK-506 is a cis-trans peptidyl-prolyl isomerase. *Nature* **1989**, *341*, 761–763.
(7) Siekerka, J. J.; Hung, S. H. Y.; Poe, M.; Lin, S. C.; Sigal, N. H. A cytosolic binding protein for the immunosuppressant FK506 has peptidyl-prolyl isomerase activity but is distinct from cyclophilin. *Nature* **1989**, *341*, 755–757.
(8) Galat, A.; Lane, W. S.; Standaert, R. F.; Schreiber, S. L. A rapamycin-selective 25-kDa immunophilin. *Biochemistry* **1992**, *31*, 2427–2434.
(9) Lander, E. S.; Lintoin, L. M.; Birren, B.; Nusbaum, C. Initial sequencing and analysis of the human genome. *Nature* **2001**, *409*, 860–921.
(10) Venter, J. C.; Adams, M. D.; Myers, E. W.; Li, P. W.; Mural, R. The sequence of the human genome. *Science* **2001**, *291*, 1304–1351.
(11) Galagan, J. E.; Calvo, S. E.; Borkovich, K. A.; Selker, E. U.; Read, N. D.; Jaffe, D.; FitzHugh, W.; Ma, L. J.; et al. The genome sequence of the filamentous fungus *Neurospora crassa*. *Nature* **2003**, *422*, 859–868.
(12) Lenhard, B.; Wahlestedt, C.; Wasserman, W. W. GeneLynx mouse: integrated portal to the mouse genome. *Genome Res.* **2003**, *13*, 1501–1504.
(13) Adams, M. D.; Celniker, S. E.; Holt, R. A.; Evans, C. A.; Gocayne, J. D.; Amanatides, P. G. et. al., The genome sequence of *Drosophila melanogaster*. *Science* **2001**, *287*, 2185–2195.
(14) Chang, J. Y.; Sehgal, S. N.; Bansbach, C. C. FK506 and rapamycin: novel pharmacological probes of the immune response. *Trends Pharmacol. Sci.* **1991**, *12*, 218–223.
(15) Sigal, N. H.; Dumont, F. Cyclosporin A, FK506, and rapamycin: pharmacologic probes of lymphocyte signal transduction. *Annu. Rev. Immunol.* **1992**, *10*, 519–560.
(16) Galat, A.; Riviere, S. *Peptidylprolyl cis/trans isomerases*; Oxford University Press: Oxford, 1998; pp 1–117.
(17) Holt, D. A.; Luengo, J. I.; Yamashita, D. S.; Oh, H. J.; Konialian, A. L.; Yen, H.-K.; Rozamus, L. W.; Brandt, M.; Bossard, M. J.; Levy, M. A.; Eggleston, D. S.; Stout, T. J.; Liang, J.; Schultz, L. W.; Clardy, J. Design, synthesis, and kinetic evaluation of high-affinity FKBP ligands, and the X-ray crystal structures of their complexes with FKBP12. *J. Am. Chem. Soc.* **1993**, *115*, 9925–9938.
(18) Dubowchik, G. M.; Vrudhula, V. M.; Dasgupta, B.; Ditta, J.; Chen, T.; Sheriff, S.; Sipman, K.; Witmer, M.; Tredup, J.; Vyas, D. M.; Verdoorn, T. A.; Bollini, S.; Vinitsky, A. 2-Aryl-2,2-difluoroacetamide FKBP12 ligands: synthesis and X-ray structural studies. *Org. Lett.* **2001**, *3*, 3987–3990.
(19) Shafiee, A.; Motamedi, H.; Dumont, F. J.; Arison, B. H.; Miller, R. R. Chemical and biological characterization of two FK506 analogs produced by targeted gene disruption in *Streptomyces* sp. MA6548. *J. Antibiot. (Tokyo)* **1997**, *50*, 418–423.
(20) Steiner, J. P.; Connolly, M. A.; Valentine, H. L.; Hamilton, G. S.; Dawson, T. M.; Hester, L.; Snyder, S. H. Neurotrophic actions of nonimmunosuppressive analogues of immunosuppressive drugs FK506, rapamycin and cyclosporin A. *Nature Med.* **1997**, *3*, 421–428.
(21) Sezen, S. F.; Hoke, A.; Burnett, A. L.; Snyder, S. H. Immunophilin ligand FK506 is neuroprotective for penile innervation. *Nature Med.* **2001**, *7*, 1073–1074.
(22) Gold, B. G.; Nutt, J. G. Neuroimmunophilin ligands in the treatment of Parkinson's disease. *Curr. Opin. Pharmacol.* **2001**, *2*, 82–86.
(23) Avramut, M.; Achim, C. L. Immunophilins in nervous system degeneration and regeneration. *Curr. Top. Med. Chem.* **2003**, *3*, 1376–1382.
(24) Sohocki, M. M.; Bowne, S. J.; Sullivan, L. S.; Blackshaw, S.; Cepko, C. L.; Payne, A. M.; Bhattacharya, S. S.; Khaliq, S.; Qasim Mehdi, S.; Birch, D. G.; Harrison, W. R.; Elder, F. F.; Heckenlively, J. R.; Daiger, S. P. Mutations in a new photoreceptor-pineal gene on 17p cause Leber congenital amaurosis. *Nat. Genet.* **2000**, *24*, 79–83.
(25) Rosner, M.; Hofer, K.; Kubista, M.; Hengstschlager, M. Cell size regulation by the human TSC tumor suppressor proteins depends on PI3K and FKBP38. *Oncogene* **2003**, *22*, 4786–4798.
(26) Crackower, M. A.; Kolas, N. K.; Noguchi, J.; Sarao, R.; Kikuchi, K.; Kaneko, H.; Kobayashi, E.; Kawai, Y.; Kozieradzki, I.; Landers, R.; Mo, R.; Hui, C. C.; Nieves, E.; Cohen, P. E.; Osborne, L. R.; Wada, T.; Kunieda, T.; Moens, P. B.; Penninger, J. M. Essential role of Fkbp6 in male fertility and homologous chromosome pairing in meiosis. *Science* **2003**, *300*, 1291–1295.
(27) Wheeler, D. L.; Church, D. M.; Federhen, S.; Lash, A. E.; Madden, T. L.; Pontius, J. U.; Schuler, G. D.; Schriml, L. M.; Sequeira, E.; Tatusova, T. A.; Wagner, L. Database resources of National Center for Biotechnology. *Nucleic Acids Res.* **2003**, *31*, 28–33.
(28) Wu, C. H.; Yeh, L. S.; Huang, H.; Arminski, L.; Castro-Alvear, J.; Chen, Y.; Hu, Z.; Kourtesis, P.; Ledley, R. S.; Suzek, B. E.; Vinayaka, C. R.; Zhang, J.; Barker, W. C. The Protein Information Resource (PIR). *Nucleic Acids Res.* **2003**, *31*, 345–347.
(29) Galat, A. A note on clustering the functionally-related paralogues and orthologues of proteins: a case of the FK506-binding proteins (FKBPs). *Comp. Biol. Chem.* **2004**, *28*, 129–140.
(30) Galat, A. Sequence diversification of the FK506-binding proteins in several different genomes. *Eur. J. Biochem.* **2000**, *267*, 4945–4959.
(31) Kyte, J.; Doolittle, R. F. A simple method for displaying the hydropathic character of a protein. *J. Mol. Biol.* **1982**, *157*, 105–132.
(32) Kyte, J. *Structure in protein chemistry*; Garland Publishing Inc.: New York and London, 1995; pp 189–194.
(33) Thompson, J. D.; Higgins, D. G.; Gibson, T. J. CLUSTAL W: improving the sensitivity of progressive multiple sequence alignment through sequence weighting position-specific gap penalties and weight matrix choice. *Nucleic Acids Res.* **1994**, *22*, 4673–4680.
(34) Henikoff, S.; Henikoff, J. G. Amino acid substitution matrices from protein blocks. *Proc. Natl. Acad. Sci. USA* **1992**, *89*, 10915–10919.
(35) Valdar, W. S. J.; Thornton, J. M. Protein-protein interfaces: analysis of amino acid conservation in homodimers. *Proteins* **2001**, *42*, 108–124.
(36) Arndt, C. *Information measures: Information and its description in science and engineering*; Springer Verlag: Berlin and Heidelberg, 2004; pp 22–84.
(37) Levitt, M.; Yona, G. Within the twilight zone: a sensitive profile-profile comparison tool based on information theory. *J. Mol. Biol.* **2002**, *315*, 1257–1275.

(38) Berman, H. M.; Henrick, K.; Nakamura, H.; Markley, J. L. The worldwide Protein Data Bank (wwPDB.: ensuring a single, uniform archive of PDB data. *Nucleic Acids Res.* **2007**, *35*, D301–D303.
(39) Galat, A. Analysis of dynamics trajectories of DNA and DNA-drug complexes. *CABIOS* **1989**, *5*, 271–278.
(40) Schulze, G. E.; Schirmer, R. H. *Principles of protein structure*; Springer Verlag: New York and Heidelberg, 1979; pp 131–148.
(41) Gunasekaran, K.; Hagler, A. T.; Gierasch, L. M. Sequence and structural analysis of cellular retonic acid-binding proteins reveals a network of conserved hydrophobic interactions. *Proteins* **2004**, *54*, 179–194.
(42) Karlin, S.; Zhu, Z.-Y. Characterization of diverse residue clusters in protein three-dimensional structures. *Proc. Natl. Acad. Sci. USA* **1996**, *93*, 8344–8349.
(43) Tsai, J.; Taylor, R.; Chothia, C.; Gerstein, M. The packing density in proteins: standard radii and volumes. *J. Mol. Biol.* **1999**, *290*, 253–266.
(44) Cornell, W. D.; Cieplak, P.; Bayly, C. I.; Gould, I. R.; Merz, K. M.; Ferguson, M.; Spellmeyer, D. C.; Fox, T.; Caldwell, J. W. Kollman, P. A. A second generation force field for the simulation of proteins, nucleic acids, and organic molecules. *J. Am. Chem. Soc.* **1995**, *117*, 5179–5197.
(45) Hopfinger, A. J. *Conformational properties of macromolecules*; Academic Press: New York and London, 1973; pp 38–131.
(46) Liu, J.; Farmer, J. D.; Lane, W. S.; Friedman, J.; Weissman, I.; Schreiber, S. L. Calcineurin is a common target of cyclophilin-cyclosporin A and FKBP-FK506 complexes. *Cell* **1991**, *66*, 807–815.
(47) Stoddard, B. L.; Flick, K. E. Calcineurin-immunosuppressor complexes. *Curr. Opinion Struct. Biol.* **1996**, *6*, 770–775.
(48) Kunz, J.; Henriquez, R.; Schneider, U.; Deuter-Reinhard, M.; Movva, R. N.; Hall, M. N. Target of rapamycin in yeast, TOR2, is an essential phosphatidylinositol kinase homolog required for G_1progression. *Cell* **1993**, *73*, 585–596.
(49) Brown, E. J.; Albers, M. W.; Shin, T. B.; Ichikawa, K.; Keith, C. T.; Lane, W. A.; Schreiber, S. L. A mammalian protein targeted by G1-arresting rapamycin-receptor complex. *Nature* **1994**, *369*, 756–758.
(50) Sabers, C. J.; Martin, M. M.; Brunn, G. J.; Williams, J. M.; Dumont, F. J.; Wiederrecht, G.; Abraham, R. T. Isolation of a protein target of the FKBP12-rapamycin complex in mammalian cells. *J. Biol. Chem.* **1995**, *270*, 815–822.
(51) Wang, T.; Donahoe, P. K.; Zervos, A. S. Specific interaction of type I receptors of the TGF-β family with the immunophilin FKBP-12. *Science* **1994**, *265*, 674–676.
(52) Chen, Y. G.; Liu, F.; Massague, J. Mechanism of TGF-β receptor inhibition by FKBP12. *EMBO J.* **1997**, *16*, 3866–3876.
(53) Lehnart, S. E.; Huang, F.; Marx, S. O.; Marks, A. R. Immunophilins and coupled gating of ryanodine receptors. *Curr. Top. Med. Chem.* **2003**, *3*, 1383–1391.
(54) Cameron, A. M.; Steiner, J. P.; Roskams, A. J.; Ali, S. M.; Ronnett, G. V.; Snyder, S. H. Calcineurin associated with the inositol 1,4,5-trisphosphate receptor-FKBP12 complex modulates Ca^{2+} flux. *Cell* **1995**, *83*, 463–472.
(55) Gopalan, G.; He, Z.; Balmer, Y.; Romano, P.; Gupta, R.; Heroux, A.; Buchanan, B. B.; Swaminathan, K.; Luan, S. Structural analysis uncovers a role for redox in regulating Fkbp13, an immunophilin of the chloroplast thylakoid lumen. *Proc. Natl. Acad. Sci. USA* **2004**, *101*, 13945–13950.
(56) Meng, X.; Lu, X.; Morris, C. A.; Keating, M. T. A novel human gene FKBP6 is deleted in Williams syndrome. *Genomics* **1998**, *52*, 130–137.
(57) Peoples, R.; Franke, Y.; Wang, Y. K.; Perez-Jurado, L.; Paperna, T.; Cisco, M.; Francke, U. A physical map, including a BAC/PAC clone contig, of the Williams-Beuren syndrome--deletion region at 7q11.23. *Am. J. Hum. Genet.* **2000**, *66*, 47–68.
(58) Kuzhandaivelu, N.; Cong, Y. S.; Inouye, C.; Yang, W. M.; Seto, E. XAP2, a novel hepatitis B virus X-associated protein that inhibits X transactivation. *Nucleic Acids Res.* **1996**, *24*, 4741–4750.
(59) Ma, Q.; Whitlock, J. P. A novel cytoplasmic protein that interacts with the Ah receptor contains tetratricopeptide repeat motifs, and augments the transcriptional response to 2,3,7,8-tetrachlorodibenzo-p-dioxin. *J. Biol. Chem.* **1997**, *272*, 8878–8884.
(60) Meyer, B. K.; Pray-Grant, M. G.; Vanden-Heuvel, J. P.; Perdew, G. H. Hepatitis B virus X-associated protein 2 is a subunit of the unliganded aryl hydrocarbon receptor core complex and exhibits transcriptional enhancer activity. *Mol. Cell. Biol.* **1998**, *18*, 978–988.
(61) Lam, E.; Martin, M.; Wiederrecht, G. Isolation of a cDNA encoding a novel human FK506-binding protein homolog containing leucine zipper and tetratricopeptide repeat motifs. *Gene* **1995**, *160*, 297–302.
(62) Wang, H. Q.; Nakaya, Y.; Du, Z.; Yamane, T.; Shirane, M.; Kudo, T.; Takeda, M.; Takebayashi, K.; Noda, Y.; Nakayama, K. I.; Nishimura, M. Interaction of presenilins with FKBP38 promotes apoptosis by reducing mitochondrial Bcl-2. *Hum. Mol. Genet.* **2005**, *14*1889–1902.
(63) Edlich, F.; Weiwad, M.; Erdmann, F.; Fanghanel, J.; Jarczowski, F.; Rahfeld, J. U.; Fischer, G. Bcl-2 regulator FKBP38 is activated by Ca^{2+}-calmodulin. *EMBO J.* **2005**, *24*, 2688–2699.
(64) Fong, S.; Mounkes, L.; Liu, Y.; Maibaum, M.; Alonzo, E.; Desprez, P. Y.; Thor, A. D.; Kashani-Sabet, M.; Debs, R. J. Functional identification of distinct sets of antitumor activities mediated by the FKBP gene family. *Proc. Natl. Acad. Sci. USA* **2003**, *100*, 14253–14258.
(65) Bulgakov, O. V.; Eggenschwiler, J. T.; Hong, D. H.; Anderson, K. V.; Li, T. FKBP8 is a negative regulator of mouse sonic hedgehog signaling in neural tissues. *Development* **2004**, *131*, 2149–2159.
(66) Baughman, G.; Wiederrecht, G. J.; Campbell, N. F.; Martin, M. M.; Bourgeois, S. FKBP51, a novel T-cell-specific immunophilin capable of calcineurin inhibition. *Mol. Cell. Biol.* **1995**, *15*, 4395–4402.
(67) Yeh, W. C.; Li, T. K.; Bierer, B. E.; McKnight, S. L. Identification and characterization of an immunophilin expressed during the clonal expansion phase of adipocyte differentiation. *Proc. Natl. Acad. Sci. USA* **1995**, *92*, 11081–11085.
(68) Nuber, U. A.; Kriaucionis, S.; Roloff, T. C.; Guy, J.; Selfridge, J.; Steinhoff, C.; Schulz, R.; Lipkowitz, B.; Ropers, H. H.; Holmes, M. C.; Bird, A. Up-regulation of glucocorticoid-regulated genes in a mouse model of Rett syndrome. *Hum. Mol. Genet.* **2005**, *14*, 2247–2256.
(69) Binder, E. B.; Salyakina, D.; Lichtner, P.; Wochnik, G. M.; Ising, M. Polymorphisms in FKBP5 are associated with increased recurrence of depressive episodes and rapid response to antidepressant treatment. *Nat. Genet.* **2004**, *36*, 1319–1325.
(70) Callebaut, I.; Renoir, J. M.; Lebeau, M. C.; Massol, N.; Burny, R.; Baulieu, E.-E.; Mornon, J. P. An immunophilin that binds M_r 90,000 heat shock protein: structural features of a mammalian p59 protein. *Proc. Natl. Acad. Sci. USA* **1992**, *89*, 6270–6274.
(71) Cheung-Flynn, J.; Prapapanich, V.; Cox, M. B.; Riggs, D. L.; Suarez-Quian, C.; Smith, D. F. Physiological role for the cochaperone FKBP52 in androgen receptor signaling. *Mol. Endocrinol.* **2005**, *19*, 1654–1666.
(72) Chambraud, B.; Radanyi, C.; Camonis, J. H.; Rajkowski, K.; Schumacher, M.; Baulieu, E.-E. Immunophilins, Refsum syndrome and lupus nephritis. The peroxisomal enzyme phytanoyl-CoA α-hydroxylase is a new FKBP-associated-protein. *Proc. Natl. Acad. Sci. USA* **1999**, *96*, 2104–2109.
(73) Sinkins, W. G.; Goel, M.; Estacion, M.; Schilling, W. P. Association of immunophilins with mammalian TRPC channels. *J. Biol. Chem.* **2004**, *279*, 34521–34529.
(74) Yang, W.-M.; Yao, Y.-L.; Seto, E. The FK506-binding protein 25 functionally associates with histone deacetylase and with transcription factor YY1. *EMBO J.* **2001**, *20*, 4814–4825.
(75) Dolinski, K. J.; Heitman, J. Hmo1p, a high mobility group 1/2 homolog, genetically and physically interacts with the yeast FKBP12 prolyl isomerase. *Genetics* **1999**, *151*, 935–944.
(76) Leclercq, M.; Vinci, F.; Galat, A. Mammalian FKBP-25 and its associated proteins. *Arch. Biochem. Biophys.* **2000**, *380*, 20–28.
(77) DeLano, W. L. The PyMOL Molecular Graphics System (DeLano Scientific), San Carlos, California, USA. http://pymol.sourceforge.net/ (accessed Januanry 2006).
(78) van Duyne, G. D.; Standaert, R. F.; Karplus, P. M.; Schreiber, S. L.; Clardy, J. Structure of immunophilin-immunosuppressant complex. *Science* **1991**, *252*, 839–842.
(79) van Duyne, G. D.; Standaert, R. F.; Karplus, P. M.; Schreiber, S. L.; Clardy, J. Atomic structures of the human immunophilin FKBP-12 complexes with FK506 and rapamycin. *J. Mol. Biol.* **1993**, *229*, 105–124.
(80) Schultz, L. W.; Martin, P. K.; Liang, J.; Schreiber, S. L.; Clardy, J. Atomic structure of the immunophilin FKBP13-FK506 complex: insights into the composite binding surface for calcineurin. *J. Am. Chem. Soc.* **1994**, *116*, 3129–3130.
(81) Riviere, S.; Menez, A.; Galat, A. On the localization of FKBP25 in T-lymphocytes. *FEBS Lett.* **1993**, *315*, 247–251.
(82) Liang, J.; Hung, D. T.; Schreiber, S. L.; Clardy, J. Structure of the human 25 kDa FK506 binding protein complexed with rapamycin. *J. Am. Chem. Soc.* **1996**, *118*, 1231–1232.
(83) Somarelli, J. A.; Herrera, R. J. Evolution of the 12 kDa FK506-binding protein gene. *Biol. Cell* **2007**, *99*, 311–321.
(84) Burkhard, P.; Taylor, P.; Walkinshaw, M. D. X-ray structures of small ligand-FKBP complexes provide an estimate for hydrophobic interaction energies. *J. Mol. Biol.* **2000**, *295*, 953–962.
(85) Deivanayagam, C. C. S.; Carson, M.; Thotakura, A.; Narayana, S. V. L.; Chodavarapu, C. S. Structure of FKBP12.6 in complex with rapamycin. *Acta Crystallogr.* **2000**, *D56*, 266–271.
(86) Itoh, S.; Decenzo, M. T.; Livingston, D. J.; Pearlman, D. A.; Navia, M. A. Conformation of FK506 in x-ray structures of its complexes with human recombinant FKBP12 mutants. *Bioorg. Med. Chem. Lett.* **1995**, *5*, 1983–1987.

(87) Clackson, T.; Yang, W.; Rozamus, L.; Amara, J.; Hatada, M. H.; Rollins, C. T.; Stevenson, L. F.; Magari, S. R.; Wood, S. A.; Courage, N. L.; Lu, X.; Cerasoli, F.; Gilman, M.; Holt, D. Redesigning an FKBP-ligand interface to generate chemical dimerizers with novel specificity. *Proc. Natl. Acad. Sci. USA* **1998**, *95*, 10437–10442.
(88) Wilson, K. P.; Yamashita, M. M.; Sintchak, M. D.; Rotstein, S. H.; Murcko, M. A.; Boger, J.; Thomson, J. A.; Fitzgibbon, M. J.; Navia, M. A. Comparative x-ray structures of the major binding protein for the immunosuppressant FK506 with FK506 and rapamycin form and in complex. *Acta Crystallogr.* **1995**, *D51*, 511–521.
(89) Becker, J. W.; Rotonda, J.; Mckeever, B. M.; Chan, H. K.; Marcy, A. I.; Wiederrecht, G.; Hermes, J. D.; Springer, J. P. FK506-binding protein: three-dimensional structure of the complex with the antagonist L-685,818. *J. Biol. Chem.* **1993**, *268*, 11335–11339.
(90) Griffith, J. P.; Kim, J. L.; Kim, E. E.; Sintchak, M. D.; Thomson, J. A.; Fitzgibbon, J. M.; Fleming, M. A.; Caron, P. R.; Hsiao, K.; Navia, M. A. X-ray structure of calcineurin inhibited by the immunophilin-immunosuppressant FKBP12-FK506 complex. *Cell* **1995**, *82*, 507–522.
(91) Choi, J.; Chen, J.; Schreiber, S. L.; Clardy, J. Structure of the FKBP12-rapamycin complex interacting with the binding domain of human FRAP. *Science* **1996**, *273*, 239–242.
(92) Liang, J.; Choi, J.; Clardy, J. Refined structure of the FKBP12-rapamycin-FRB ternary complex at 2.2 Å resolution. *Acta Crystallogr. Biol. Sect.* **1999**, *D55*, 736–744.
(93) Huse, M.; Chen, Y.-G.; Massagué, J.; Kuriyan, J. Crystal structure of the cytoplasmic domain on the type I TGF-β receptor in complex with FKBP12. *Cell* **1999**, *96*, 425–436.
(94) Fulton, K. F.; Jackson, S. E.; Buckle, A. M. Energetic and structural analysis of the role of tryptophan 59 in FKBP12. *Biochemistry* **2003**, *42*, 2364–2372.
(95) Becker, J. W.; Rotonda, J.; Cryan, J. G.; Martin, M.; Parsons, W. H.; Sinclair, P. J.; Wiederrecht, G.; Wong, F. 32-Indolyl ether derivatives of ascomycin: three-dimensional structures of complexes with FK506-binding protein. *J. Med. Chem.* **1999**, *42*, 2798–2804.
(96) Walker, J. R.; Davis, T.; Newman, E. M.; Finerty, P.; Mackenzie, F.; Weigelt, J.; Sundstrom, M.; Arrowsmith, C.; Edwards, A.; Bochkarev, A.; Dhe-Paganon, S. Structure of the human FK506 binding protein-8. http://www.rcsb.org/pdb (accessed August 2007).
(97) Sinars, C.; Cheung-Flynn, J.; Rimerman, R. A.; Scammell, J. G.; Smith, D. F.; Clardy, J. Structure of the large FK506-binding protein FKBP51, an Hsp90-binding protein and a component of steroid receptor complex. *Proc. Natl. Acad. Sci. USA* **2003**, *100*, 868–873.
(98) Wu, B.; Li, R.; Liu, Y.; Lou, Z.; Ding, Y.; Shu, C.; Ye, S.; Bartlam, M.; Shen, B.; Rao, Z. 3D structure of human FK506-binding protein 52: implications for the assembly of the glucocorticoid receptor/Hsp90/immunophilin heterocomplex. *Proc. Natl. Acad. Sci. USA* **2004**, *101*8348–8353.
(99) Li, S.; Finley, J.; Luan, C-H.; Qiu, S.; Gray, R.; Shang, Q.; Luo, D.; Hongli, C.; Zhao J., Huang, W-Y.; Delucas, L. J.; Nagy, L.; Stanton, A.; Luo, M.; Symersky, J.; Schormann, N.; Lin, J.; Tsao, Johnson, D. H.; Carson, G. W. M. Structural genomics of C.elegans: FKBP-type peptidylprolyl isomerase. http://www.rcsb.org/pdb (accessed August 2007).
(100) Weiergraber, O. H.; Eckhoff, A.; Granzin, J. Crystal structure of a plant immunophilin domain involved in regulation of mdr-type abc transporters. *FEBS Lett.* **2006**, *580*, 251–255.
(101) Granzin, J.; Eckhoff, A.; Weiergraber, O. H. Crystal structure of a multi-domain immunophilin from Arabidopsis thaliana: a paradigm for regulation of plant ABC transporters. *J. Mol. Biol.* **2006**, *364*, 799–809.
(102) Rotonda, J.; Burbaum, J. J.; Chan, H. K.; Marcy, A. I.; Becker, J. W. Improved calcineurin inhibition of yeast FKBP12-drug complexes. *J. Biol. Chem.* **1993**, *268*, 7607–7609.
(103) Riboldi-Tunnicliffe, A.; Konig, B.; Jessen, S.; Weiss, M. S.; Rahfeld, J.; Hacker, J.; Fischer, G.; Hilgenfeld, R. Crystal structure of mip, a prolylisomerase from Legionella pneumophila. *Nat. Struct. Biol.* **2001**, *8*, 779–783.
(104) Saul, F. A.; Arie, J.-P.; Vulliez-Le Normand, B.; Kahn, R.; Betton, J.-M.; Bentley, G. A. Structural and functional studies of FKBP from *Escherichia coli*, a cis/trans peptidyl-prolyl isomerase with chaperone activity. *J. Mol. Biol.* **2004**, *335*, 595–608.
(105) Suzuki, R.; Nagata, K.; Yumoto, F.; Kawakami, M.; Nemoto, N.; Furutani, M.; Adachi, K.; Maruyama, T.; Tanokura, M. Three-dimensional solution structure of an archaeal FKBP with a dual function of peptidyl prolyl cis-trans isomerase and chaperone-like activities. *J. Mol. Biol.* **2003**, *328*, 1149–1160.
(106) Weiwad, M.; Edlich, F.; Kilka, S.; Erdmann, F.; Jarczowski, F.; Dorn, M.; Moutty, M.-C.; Fischer, G. Comparative analyses of calcineurin inhibition by complexes of immunosuppressive drugs with human FK506 binding proteins. *Biochemistry* **2006**, *45*, 15776–15784.
(107) Itoh, S.; Navia, M. A. Structure comparison of native and mutant human recombinant FKBP12 complex with the immunosuppressant drug FK506 (tacrolimus). *Protein Sci.* **1995**, *4*, 2261–2268.
(108) Cheng, J.-W.; Lepre, C.; Moore, J. M. ^{15}N NMR relaxation studies of the FK506 binding proteins: dynamic effect of ligand binding and implications for calcineurin recognition. *Biochemistry* **1994**, *33*, 4093–4100.
(109) Kissinger, C. R.; Parge, H. E.; Knighton, D. R.; Lewis, C. T.; Pelletier, L. A.; Tempczyk, A.; Kalish, V. J.; Tucker, K. D.; Showalter, R. E.; Moomaw, E. W.; Gastinel, L. N.; Habuka, N.; Chen, X.; Maldonaldo, F.; Barker, J. E.; Bacquet, R.; Villafranca, J. E. Crystal structures of human calcineurin and the human FKBP12-FK506-calcineurin complex. *Nature* **1995**, *378*, 641–644.
(110) Abraham, R. T.; Wiederrecht, G. J. Immunopharmacology of rapamycin. *Annu. Rev. Immunol.* **1996**, *14*, 483–510.
(111) Galat, A. Involvment of some large immunophilins and their ligands in the protection and regeneration of neurons: a hypothetical mode of action. *Comp. Biol. Chem.* **2006**, *30*, 348–359.
(112) Nakanishi, I.; Fedorov, D. G.; Kitaura, K. Molecular recognition mechanism of FK506 binding protein: an all-electron fragment molecular orbital study. *Proteins* **2007**, *68*, 145–158.
(113) Orengo, C. A.; Thornton, J. M. Protein families and their evolution - a structural perspective. *Annu. Rev. Biochem.* **2005**, *74*, 867–900.
(114) Sormani, R.; Yao, L.; Menand, B.; Ennar, N.; Lecampion, C.; Meyer, C.; Robaglia, C. Saccharomyces cerevisie FKBP12 binds *Arabodopsis thaliana* TOR and its expression in plants leads to rapamycin sensitivity. *BMC Plant Biol.* **2007**, *7*, 26.
(115) Harrison, R. K.; Stein, R. L. Mechanistic studies of enzymatic and nonenzymatic prolyl cis-trans isomerization. *J. Am. Chem. Soc.* **1992**, *114*, 3464–3471.
(116) Ke, H.; Mayrose, D.; Cao, W. Crystal structure of cyclophilin A complexed with substrate Ala-Pro suggests a solvent-assisted mechanism of cis-trans isomerization. *Proc. Natl. Acad. Sci. USA* **1993**, *90*, 3324–3328.
(117) Hur, S.; Bruice, T. C. The mechanism of cis-trans isomerization of prolyl peptides by cyclophilin. *J. Am. Chem. Soc.* **2002**, *124*, 7303–7313.
(118) Agarwal, P. K.; Geist, A.; Gorin, A. Protein dynamics and enzymatic catalysis: investigating the peptidyl-prolyl cis-trans isomerization activity of cyclophilin A. *Biochemistry* **2004**, *43*, 10605–10618.
(119) Li, G.; Cui, Q. What is so special about Arg 55 in the catalysis of cyclophilin A? insights from hybrid QM/MM simulations. *J. Am. Chem. Soc.* **2003**, *125*, 15028–15038.
(120) Eisenmesser, E. Z.; Millet, O.; Labeikovsky, W.; Korzhnev, D. M.; Wolf-Watz, M.; Bosco, D. A.; Skalicky, J. J.; Kay, L. E.; Kern, D. Intrinsic dynamics of an enzyme underlies catalysis. *Nature* **2005**, *438*, 117–121.
(121) Trzesniak, D.; van Gunsteren, W. F. Catalytic mechanism of cyclophilin as observed in molecular dynamics simulations: pathway prediction and reconciliation of X-ray crystallographic and NMR solution data. *Protein Sci.* **2006**, *15*, 2544–2551.
(122) Albers, M. W.; Walsh, C. T.; Schreiber, S. L. Substrate specificity for the human rotamase FKBP: A view of FK506 and rapamycin as leucine-(twisted amide.-proline mimics. *J. Org. Chem.* **1990**, *55*, 4984–4986.
(123) van Gunsteren, W. F.; Berendsen, H. J. C. Computer simulations of molecular dynamics: methodology, applications, and perspectives in chemistry. *Angw. Chem. Int. Ed.* **1990**, *29*, 992–1023.
(124) Hansson, T.; Oostenbrink, C.; van Gunsteren, W. F. Molecular dynamics simulations. *Curr. Opin. Struct. Biol.* **2002**, *12*, 190–196.
(125) Warshel, A. *Computer modeling of chemical reactions in enzymes and solutions*; J. Wiley & Sons: New York, 1997; pp 1–256.
(126) Bren, M.; Florian, J.; Mavri, J.; Bren, M. Do all pieces make a whole? Thiele cumulants and the free energy decomposition. *Theor. Chem. Acc.* **2007**, *117*, 535–540.
(127) De Groot, B. L.; Grubmuller, H. Water permeation across biological membranes: mechanism and dynamics of aquaporin-1 and GlpF. *Science* **2001**, *294*, 2353–2357.
(128) Bernèche, S.; Roux, B. Energetics of ion conductance through the K^+ channel. *Nature* **2001**, *414*, 73–77.
(129) Galat, A.; Stura, E.; Thai, R.; Guimiot, F.; Simonneau, M. X-ray structure of the C-terminal of rapamycin-binding domain of murine FKBP25, unpublished data.

CI700429N